2009 IEEE International Conference on Robotics and Automation
Kobe International Conference Center
Kobe, Japan, May 12-17, 2009

A Compact Soft Actuator Unit for Small Scale Human Friendly Robots

N.G.Tsagarakis[1], Matteo Laffranchi[1], Bram Vanderborght[1,2] and D.G.Caldwell[1]

[1]Italian Institute of Technology (IIT), Genova 16163, Italy

[2]University of Brussels, B-1050 Brussels, Belgium

Abstract— **This paper presents the development of a new compact soft actuation unit intended to be used in multi degree of freedom and small scale robotic systems such as the child humanoid robot "iCub" [1]. Compared to the other existing series elastic linear or rotary implementations the proposed design shows high integration density and wider passive deflection. The miniaturization of the newly developed high performance unit was achieved with a use of a new rotary spring module based on a novel arrangement of linear springs.**

The model and the control scheme of the actuator are analysed. The proposed control scheme is a velocity based controller that generates command signals based on the desired simulated stiffness using the spring deflection state. The overall system is evaluated with experimental trials performed using a prototype unit.

Preliminary results are presented to show that the unit and the proposed control scheme are capable of replicating virtual impedances within a wide range and with good fidelity.

I. Introduction

UNTIL the last decade, the main approach in robotic actuation was the use of heavy, stiff position/velocity and torque actuation units coupled with rigid non back-drivable transmission mechanisms. These robots are optimised for precision and speed and are highly repeatable, acting within constrained and well defined environments and are therefore suitable for conventional industrial automation. However, as the areas for technical exploitation have been increased, new demands are placed on the available actuation systems and it has become increasingly clear that this traditional stiff actuation approach has significant performance limitations related to safety, efficiency and the ability to interact with the environment. The ability of the stiff actuation units to safely interact with their surroundings can be increased by means of software techniques based on impedance/admittance regulation and joint torque control [2-4], however, the existence of delays at all stages of the software system make these conventionally stiff actuated systems unsafe during fast impacts and generally incapable of managing high-speed contact transients

To address this problem a wide range of experimental novel compliant actuation systems have been developed during the past fifteen years. The series elastic actuator family is an early development towards the realization of actuator units with inherent compliance [5-8]. This actuator employs a fixed compliance element between a high impedance actuator and the load. The elastic element used in most realizations is based on the use of torsion/die linear springs or viscoelastic materials usually combined with ball screw reduction drives (linear SEA) or planetary gearbox and cable assemblies (rotary systems). Revolute actuators have been also produced using "X shaped" cross section metal torsion springs or even rubber balls held between alternating teeth [9]. Although providing successful solutions these designs are relatively big (ball screw and die springs or cables and extension springs arrangements) or suffer from small passive deflection ranges (designs using torsion springs).

Actuation units with the ability to modulate compliance have also been developed [10-19]. These variable compliance actuation systems typically employ two actuator units in combination with passive stiffening elastic elements to control, independently, the compliance and the equilibrium position of the actuated joint.

Obvious advantages that the variable stiffness implementations offer when compared with the fixed passive compliance units are the ability to regulate stiffness and position independently and the wide range of stiffness and energy storage capabilities. On the other hand the mechanical complexity, size, weight, cost and integration are still open issues in variable passive compliance realizations. As a result their application to multi degree of freedom or small scale robotic machines still remains a challenging task.

N.G.Tsagarakis is with the Italian institute of Technology (IIT), Genova 16163, Italy (phone: +39 010 71781 428; e-mail: nikos.tsagarakis@ iit.it).
Matteo Laffrangi is with the Italian institute of Technology (IIT), Genova 16163, Italy (e-mail: Matteo.Laffranchi@ iit.it).
Bram Vanderborght is with the Italian institute of Technology (IIT), Genova 16163, Italy (e-mail: Bram.Vanderborght @ iit.it) and within the University of Brussels, Belgium.
D.G.Caldwell is with the Italian institute of Technology (IIT), Genova 16163, Italy (e-mail: darwin.caldwell@ iit.it).

In this instance, the SEA family clearly has an advantage when compared with the variable stiffness implementations. In addition, its main disadvantage of the preset passive mechanical compliance can be at some degree minimized by combining the unit with active stiffness control.

This work was motivated by the need for a soft highly integrated actuation unit suitable for small scale multi degree of freedom robots. In particular the actuator was developed for the new generation of the "iCub" robot, a child sized humanoid (1m height) with 53 D.O.F developed in [1].

Based on the above comparison between the fixed and variable compliance units it is seen that a fixed compliance actuator was the most realistic choice for the "iCub".

In this paper we present the realization of a new compact rotary series elastic actuator. The actuator shows particular improvements over the existing implementations based on ball-screw/die spring, torsion springs or extension springs/cable assemblies. The compact design of the actuator is due to the novel mechanical implementation of the compliant module. Despite its small size, the actuator still retains a high level of performance and it is a potential generic solution for small scale mutli-degree of freedom systems where compliance is also desired. We show that by combining the passive compliance of this unit with active compliance control based on velocity regulation a wide range of compliance adjustment can also be obtained.

In this paper section II focuses on the description of the actuator mechanical design while section III presents the stiffness model of the compliant module. The overall dynamic model and control of the actuator follow in section IV while V shows experimental results for the performance of the actuator and section VI addresses the conclusions.

II. THE MECHANICS OF THE COMPACT SOFT ACTUATION UNIT

The mechanical realization of a soft actuation unit is based on the serial elastic actuator concept, but particular attention has been paid to satisfying the dimensional and weight requirements of the "iCub" robot [1].

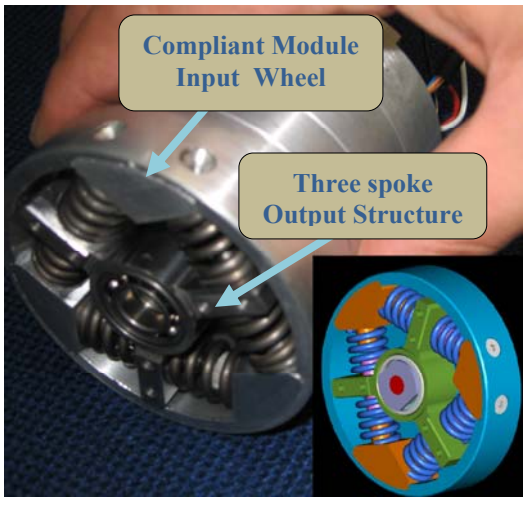

Fig. 1 The prototype of the compact SEA module.

The high integration density is due to the novel mechanical compliant module. To minimize dimensions while achieving high rotary stiffness a mechanical structure with a three spoke output component, a circular input pulley and six linear springs has been designed and fabricated.

The circular component forms the input of the compliant module and is fixed to the output of the reduction drive. The three spoke element rotates on bearings with respect to the circular base and is coupled with it by means of six springs, Figure 1. The three spoke component forms the output of the compliant module and the mounting base of the output link.

The six linear springs when inserted in the arrangement shown in Figure 1 experience a pre-contraction equal to half of the maximum acceptable deflection. Deflections larger than the maximum allowable are not permitted by mean of mechanical pin based locks.

Two 12bit absolute position sensors are integrated within the actuation group measuring respectively the mechanical angle of the motor after the reduction drive and the deflection angle of the compliant module. These sensors not only allow the monitoring of the link position but also allow the evaluation of the joint torque. Because of the compliance introduced it is possible to use the sensor measuring the compliant module deflection to estimate the torque.

III. COMPLIANCE MODULE STIFFNESS MODEL

In this section the stiffness model of the three spoke spring structure is presented. The deflection of the compliant module results in torques through compression of the spring elements along their main axis, Figure 2.

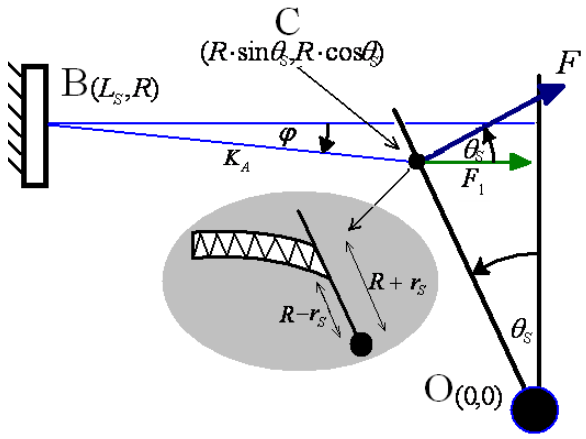

Fig. 2 Compression of the spring as a result of the module deflection.

Considering one of the antagonist linear spring pairs in Figure 3, the axial forces generated by each of the springs when the compliant three spoke module is deflected from the equilibrium position by an angle of θ_S is given by

$$F_1 = K_A \cdot (x_p + x(\theta_S)),\ F_2 = K_A \cdot (x_p - x(\theta_S)) \qquad (1)$$

where x_p is the spring pre-contraction and $x(\theta_S) = R \cdot \sin\theta_S$ is the resulted deflection of the two springs

along their main axis, K_A is the spring axial stiffness and R the length of the spoke arm. The combined axial force applied in any spoke is therefore:

$$F = F_1 - F_2 = 2 \cdot K_A \cdot R \cdot \sin \theta_S \quad (2)$$

The corresponding torque generated at the joint because of the axial forces of one antagonistic pair of springs is equal to

$$T = F \cdot R \cdot \cos \theta_S = 2 \cdot K_A \cdot R^2 \cdot \sin \theta_S \cdot \cos \theta_S \quad (3)$$

So far we consider that the axial spring force is concentrated at one point. Considering that the spring has an external radius of r_S, Figure 2 shows that the axial spring compression is not equal for the whole surface area in contact with the spoke. The areas farthest from the centre of rotation are subject to larger deflections creating higher forces.

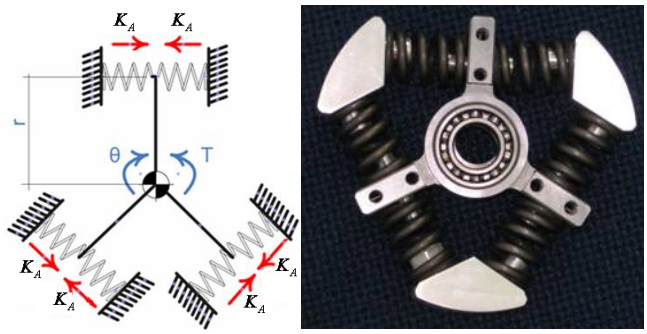

Fig. 3 The three spoke spring coupling arrangement.

As a result the torque generated by the axial deflection of the antagonistic pair of springs can be computed by

$$T = \frac{1}{2 \cdot r_S} \int_{R-r_s}^{R+r_s} 2 \cdot K_A \cdot R^2 \cdot \sin \theta_S \cdot \cos \theta_S dR = \quad (4)$$

$$2 \cdot K_A \cdot (R^2 + \frac{r_S^2}{3}) \cdot \sin \theta_S \cdot \cos \theta_S$$

Thus, the combined torque at the joint considering the axial forces from all three pairs is

$$T_{Total} = 3 \cdot T = 6 \cdot K_A \cdot (R^2 + \frac{r_S^2}{3}) \cdot \sin \theta_S \cdot \cos \theta_S \quad (5)$$

By differentiating (5), the rotary stiffness of the three spoke module, due to the axial deflection of the springs is

$$K_S = \frac{dT_{Total}}{d\theta_S} = 6 \cdot K_A \cdot (R^2 + \frac{r_S^2}{3}) \cdot (2 \cdot \cos \theta_S^2 - 1) \quad (6)$$

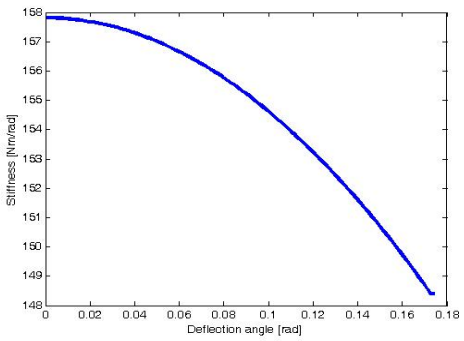

Fig. 4 The stiffness profile of the compliant module.

Figure 4 shows the theoretical stiffness of the module within the range of the deflection angle, for the first prototype module with the following parameters ($K_A = 62KN/m, R = 20.5mm, r_S = 6.3mm$). It can be seen that the stiffness is slightly reduced as the deflection angle increases (notice that y axis does not start from zero).

IV. ACTUATION UNIT DYNAMICS AND CONTROL

The actuator consists of three main components, a brushless DC motor, a harmonic reduction drive and the rotary compliant module outlined above. These components can be represented by the mechanical model in Figure 5.

The model is composed of the rotary inertia and viscous damping of the motor J_M, D_M, the gear drive with the reduction ratio of N, the elastic module with an equivalent spring constant of K_s (equation 6), the output link inertia and axial damping coefficient J_L, D_L.

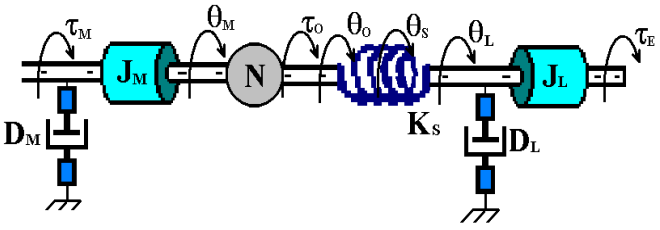

Fig. 5 Compact SEA mechanical model diagram.

In addition, θ_M, θ_O are the motor mechanical angles before and after the reduction drive, θ_L is the angle of the output link and θ_S is the rotary defection of the elastic module with respect to θ_O such as that $\theta_L = \theta_O + \theta_S$.

Finally, τ_M is the torque provided by the actuator while τ_O is the input torque of the elastic element and τ_E is the torque imposed to the system by the load and/or the environment.

The above system can be described by the following set of dynamic equations.

$$(J_M \cdot N^2 \cdot s^2 + D_M \cdot N^2 \cdot s + K_S) \cdot \theta_O - K_S \cdot \theta_L = \tau_O \quad (7)$$

$$(J_L \cdot s^2 + D_L \cdot s + K_S) \cdot \theta_L - K_S \cdot \theta_O = \tau_E \quad (8)$$

In the case of absence of active compliance control (ie a stiff position controlled actuator) we can consider $\dot{\theta}_O = 0$ and the output impedance of the system can be obtained by differentiating (8) and dividing both sides by $\dot{\theta}_L$. Thus the impedance of the system at the output can be shown to be equal to

$$Z_E = \frac{d\tau_E}{d\theta_L} = (J_L \cdot s^2 + D_L \cdot s + K_S) \quad (9)$$

Equation (9) says that what we will feel is a combination of the passive compliance together with the inertia and damping properties of the system. For fast contacts/impacts the inertial forces dominate and are the ones that a user interacting with the output link will feel more. To regulate the above preset impedance, in higher or lower values, as may be required by particular interaction properties we use an active compliance control scheme to regulate the overall link deflection produced by the applied load. A velocity based controller is used to achieve this by by regulating $\dot{\theta}_O$.

Incorporating $\dot{\theta}_O$, the impedance expression, (9) becomes

$$Z_E = \frac{d\tau_E}{d\theta_L} = (J_L \cdot s^2 + D_L \cdot s + K_S) - K_S \cdot \frac{d\theta_O}{d\theta_L} \quad (10)$$

To make the actuator output follow a desired simulated impedance, equation (11) below must be applied.

$$Z_D = \frac{d\tau_E}{d\theta_L} \quad (11)$$

Where $Z_D(s)$ is the desired simulated impedance of the actuator. The above equation defines the desired characteristics of the actuator motion/torque to replicate a specific compliant behaviour. Having specified this behaviour the control law for the desired $\dot{\theta}_O$ can be derived by equating (10) and (11) and solving with respect to $\dot{\theta}_O$.

$$Z_D = (J_L \cdot s^2 + D_L \cdot s + K_S) - K_S \cdot \frac{d\theta_O}{d\theta_L} \quad (12)$$

or $$Z_D \cdot \dot{\theta}_L = (J_L \cdot s^2 + D_L \cdot s + K_S) \cdot \dot{\theta}_L - K_S \cdot \dot{\theta}_O \quad (13)$$

By substituting $\theta_L = \theta_O + \theta_S$ and solving for $\dot{\theta}_O$ the final control law for the motor velocity as a function of the deflection velocity of the compliant element $\dot{\theta}_S$ can be derived.

$$\dot{\theta}_O = \left(\frac{K_S}{-J_L \cdot s^2 - D_L \cdot s + Z_D} - 1\right) \cdot \dot{\theta}_S \quad (14)$$

The above equation describes only the portion of the desired velocity trajectory for θ_O which is responsible for the replication of a specific compliant behaviour at the output of the actuation unit.

In addition, the term $\dot{\theta}_{TD}$ can be superimposed in equation (14) to represent the desired velocity trajectory of the output motion. Therefore the overall velocity trajectory $\dot{\theta}_{OD}$ can be written as

$$\dot{\theta}_{OD} = \dot{\theta}_{TD} + \left(\frac{K_S}{-J_L \cdot s^2 - D_L \cdot s + Z_D} - 1\right) \cdot \dot{\theta}_S \quad (15)$$

A block diagram of the active control scheme expressed by equation (15) is shown in Figure 6, with the "Compliance Regulation Filter" being used to implement equation (14).

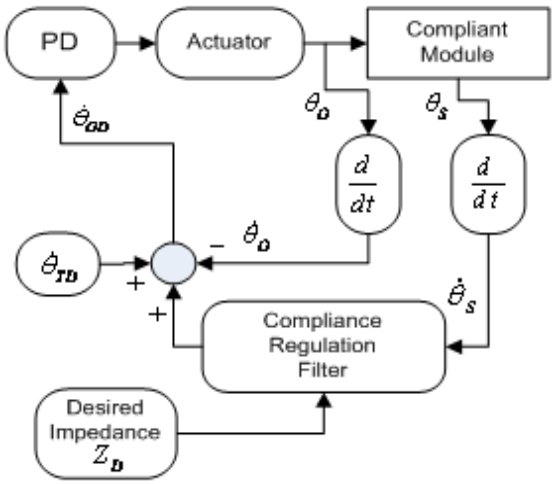

Fig. 6 Schematic of the active compliance control scheme.

V. SYSTEM EXPERIMENTAL EVALUATION

Experiments were conducted to evaluate the ability of the velocity based control scheme, and the actuation unit to regulate the output impedance for values different from the preset mechanical values. In these experiments only the tuning of the stiffness component of the output impedance is considered leaving the other inertial and damping components unaffected. The experiments were performed using the prototype actuation unit shown in Figure 7.

For the first prototype, six linear springs made of 2.2mm C85 Carbon Steel wire were used. The springs have a stiffness of 62kN/m, a free length of 18mm and a maximum allowable deflection of 6mm. When inserted as shown in Figure 1, the springs experience a pre-contraction of 3mm which is half of the acceptable deflection. Mechanical pin based locks prevent the spring overloading by limiting the maximum deflection to 6mm. This gives a total rotary deflection range of $\pm = 0.18 rad$. Given the stiffness of the compliant module this deflection is considered sufficient for the motor groups used in the humanoid robot iCub [1]. These motors produce a peak torque ranging from 20Nm-40Nm.

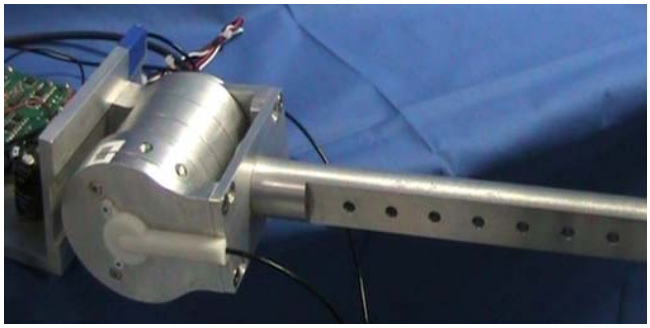

Fig. 7 The prototype of the compact compliant unit.

The actuator of the unit was formed by the combination of a Kollmorgen RBE1211 frameless brushless motor capable of providing 0.8Nm of torque, with a harmonic drive CSD 17 having a reduction ratio of N=100 and a peak rated torque of 40Nm. The inertia and viscous damping parameters of the motor are $J_M = 8.47 \cdot 10^{-6} Kg \cdot m^2, D_M = 19.68 \cdot 10^{-6} \frac{Nm \cdot Sec}{rad}$

The output of the unit was connected to a link with a mass and inertia of $M_L = 1.6Kg$ and $J_L = 5 \cdot 10^{-4} Kg \cdot m^2$ respectively. The overall dimensions of the compact prototype compliant unit together with its technical specifications are illustrated in Table 1.

TABLE 1 SPECIFICATIONS OF THE COMPLIANT ACTUATOR

Diameter	70mm
Length	80mm
Power	190W
Gear Ratio	100:1
Peak Torque	40Nm
Max Rotary Passive Deflection	+/-0.18rad
Weight	0.52Kg

The unit controller and power driver are custom control boards based on the Motorola DSP 56F8000 chip with a CAN communication interface.

In the first experiment different desired stiffness values were used to evaluate the ability of the system to realize compliances of varying amplitude. In these trials the equilibrium position of the motor was fixed to a certain angle ($\dot{\theta}_{TD} = 0$). Data for two cases are presented below. In the first case, Figure 8, the unit was commanded to retain a certain position when unperturbed and to work as an impedance source with a simulated stiffness component of 30Nm/rad when a load is applied to the output link. That is 6 times smaller than the maximum mechanical passive stiffness of the joint (see Figure 4). The top graph in Figure 8 depicts the stiffness regulation performance. Note on the third graph from the top the motor motion (blue line) shows the motor working towards the direction of the applied torque. This generates the required overall link deflection (purple line) in order to satisfy the commanded simulated stiffness.

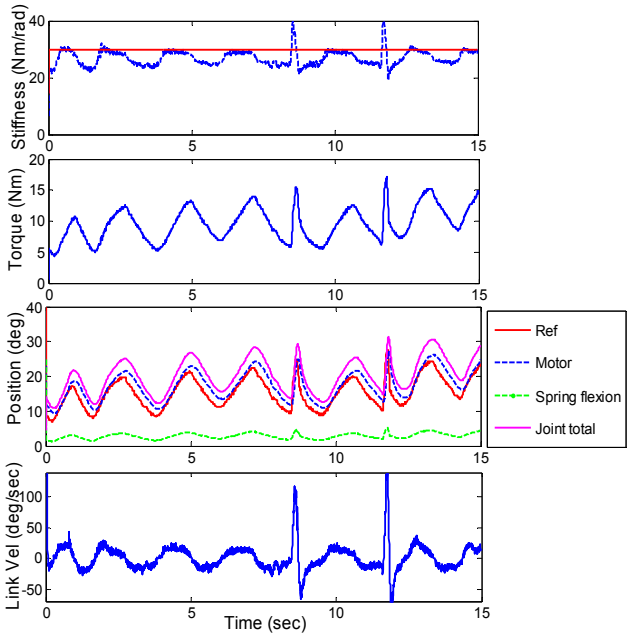

Fig. 8 Simulated spring component of 30Nm/rad.

In the second case, Figure 9, the desired simulated stiffness was set equal to 600Nm/rad (4 times the maximum mechanical preset stiffness). The third graph shows that the motion generated by the motor works in antagonism with the applied load to produce an reverse displacement (blue line) that compensates the deflection of the passive spring element (green lane). This reduces the overall link displacement (purple line) as seen by the user that applies the load.

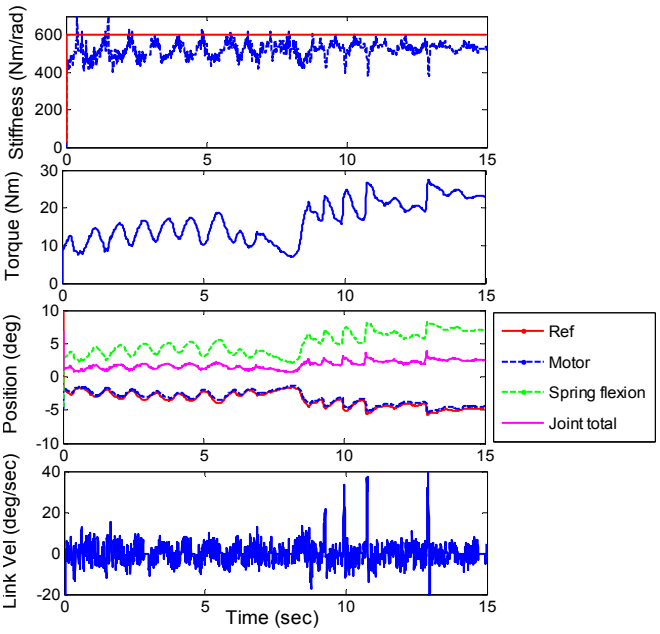

Fig. 9 Simulated spring component of 600Nm/rad.

For both the low and high stiffness case the spikes on the simulated compliance (blue line, top graph) in Figures 8, 9

reveal the tendency of the actuator to display the mechanical preset stiffness during high rate perturbations. These actions cannot normally be addressed by the bandwidth of the controller.

Following the above, the behaviour of the actuator and its control under accidental impacts for different values of the simulated stiffness were observed. In these trials the motor was commanded to follow a sinusoidal trajectory with a frequency of 0.8Hz while accidental collisions were randomly generated within the range of motion of the link. Two desired stiffness values were examined and were set equal to those in the stiffness regulation experiment ($K_S = 30Nm/rad$ and $K_S = 600Nm/rad$)

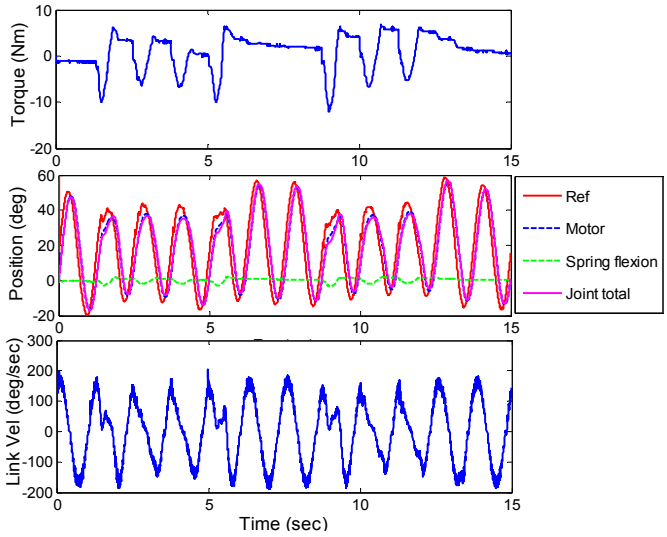

Fig. 10 Collisions of the link for a simulated stiffness of 30Nm/rad.

Results of the first case ($K_S = 30Nm/rad$), shows the ability of the system to absorb the impact by effectively modulating the reference sinusoidal trajectory (red line) of the motor in Figure 10.

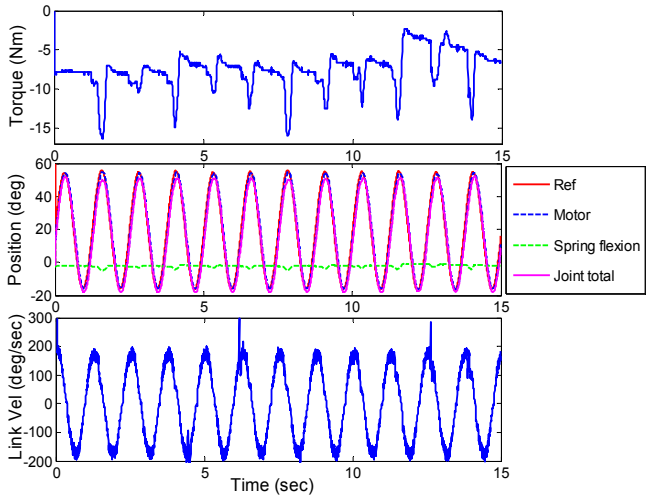

Fig. 11 Collisions of the link for a simulated stiffness of 600Nm/rad.

In the case of the high simulated stiffness it can be observed in Figure 11 that the high simulated stiffness does not allow the regulation of the sinusoidal trajectory when the collisions occur. The stiffness modulation term of equation (15) is not large enough to adapt the sinusoidal reference motion trajectory term $\dot{\theta}_{TD}$ during the collision phase. The result of this high actuator stiffness is the higher torques measured during the impact compared to the ones for the low virtual stiffness

VI. CONCLUSIONS AND FURTHER WORK

In this work the design of a new compact soft actuator which forms the actuation means for a small, multi degree of freedom robot (iCub) is presented. The miniaturization of the high performance unit was achieved using a novel rotary spring module realized by 6 linear springs arranged to constrain the motion of a three spoke structure which rotates relatively to the reduction drive output and acts as a mounting basement for the output link.

The model and control scheme for the actuator were analysed and a velocity based controller proposed that generates velocity commands based on the desired virtual stiffness using the spring deflection state. The overall system was evaluated with experimental trials performed using a prototype unit.

The preliminary results obtained from these experiments show that the unit and the proposed control scheme are capable of replicating simulated impedances within a wide range with good fidelity. Additional studies will include further development of the control scheme to incorporate a stiffness adaptation agent to allow self tuning of the stiffness according to the safety and task performance needs, using the state measurements of the system.

ACKNOWLEDGMENT

This work is supported by the VIACTORS European Commission FP7-ICT-2007-3 project.

REFERENCES

[1] N.G.Tsagarakis, G.Metta, G.Sandini, D.Vernon, R.Beira, F.Becchi, L.Righetti, J.S.Victor, A.J. Ijspeert, M.C.Carrozza and D.G.Caldwell, "iCub –The Design and Realization of an Open Humanoid Platform for Cognitive and Neuroscience Research", Advanced Robotics, Vol.21, No.10, pp, 1151-1175, 2007.

[2] Vischer D. and Kathib O., "Design and development of high-performance torque-controlled joints," IEEE Trans. Robot. Automation, 1995, vol. 11, pp. 537–544.

[3] Hirzinger G., Sporer N., Albu-Schaffer A., Hahnle M., Krenn R., Pascucci A., and Schedl M., "DLR's torque-controlled light weight robot III – are we reaching the technological limits now?", Proceedings of IEEE International Conference on Robotics and Automation, 2002, vol. 2, pp. 1710–1716.

[4] Sang-Ho Hyon, Hale, J.G., Cheng, G., "Full-Body Compliant Human–Humanoid Interaction: Balancing in the Presence of Unknown External Forces", IEEE Transactions on Robotics and Automation, 2007, vol. 23, Issue 5, pp. 884 – 898.

[5] Jerry Pratt and Gill Pratt, "Intuitive control of a planar bipedal walking robot", International Conference on Intelligent Robots and Systems, 1998, pp2014-2021.

[6] Rodney A. Brooks, Cynthia Breazeal, Matthew Marjanovic, Brian Scassellati, and Matthew Williamson, The Cog Project: Building a Humanoid Robot, Springer-Verlag,1999, To appear in a Springer-Verlag Lecture Notes in Computer Science Volume.
[7] Kazuo Hirai, Masato Hirose, Yuji Haikawa, and Toru Takenaka, "The development of honda humanoid robot", International Conference on Robotics and Automation, 1998, pp1321-1326.
[8] Pratt G. and Williamson M., "Series elastic actuators", Proceedings of IEEE/RSJ International Conference on Intelligent Robots and Systems, 1995, vol. 1, pp. 399–406.
[9] Gill Pratt, "Low Impedance Walking Robots", Integ. and Comp. Biol., 42:174–18,1 2002.
[10] Sugar T.G., "A Novel Selective Compliant Actuator", Mechatronics Journal, 2002, vol. 12 (9-10), pp. 1157-1171.
[11] Hurst J.W., Chestnutt J., and Rizzi A., "An Actuator with Physically Variable Stiffness for Highly Dynamic Legged Locomotion", Proceedings of the International Conference on Robotics and Automation, 2004, vol.5, pp. 4662-4667.
[12] Migliore S.A., Brown E.A., and DeWeerth S.P., "Biologically Inspired Joint Stiffness Control", Proceedings of the IEEE International Conference on Robotics and Automation 2005, pp. 4508- 4513.
[13] Tonietti G., Schiavi R. and Bicchi A., "Design and Control of a Variable Stiffness Actuator for Safe and Fast Physical Human/Robot Interaction", Proceedings of the IEEE, International Conference on Robotics and Automation, 2005, pp. 526- 531.
[14] Van Ham R, Vanderborght B.,Van Damme M., Verrelst B., and Lefeber D., "MACCEPA, the mechanically adjustable compliance and controllable equilibrium position actuator: Design and implementation in a biped robot", Robotics and Autonomous Systems, 2005 vol.55, nr. 10, pp. 761-768.
[15] Koganezawa K., Nakazawa T., Inaba T., "Antagonistic Control of Multi-DOF Joint by Using the Actuator with Non-Linear Elasticity", Proceedings of the IEEE, International Conference on Robotics and Automation, 2006, pp 2201-2007.
[16] Hollander K.W., Sugar T.G., and Herring D.E., "A Robotic 'Jack Spring' For Ankle Gait Assistance", Proceedings CIE 2005, ASME 2005 International Design Engineering Technical Conferences 2005, California, USA, pp. 24-28.
[17] Wolf S. Hirzinger G., "A new variable stiffness design: Matching requirements of the next robot generation", Proceedings of the International Conference on Robotics and Automation, 2008, pp 1741-1746.
[18] R. Schiavi, G. Grioli, S. Sen, A. Bicchi, " VSA-II: a Novel Prototype of Variable Stiffness Actuator for Safe and Performing Robots Interacting with Humans", Proceedings of the International Conference on Robotics and Automation, 2008, pp 2171-2176.
[19] Morita T., Sugano S., "Development of 4-DOF Manipulator Using Mechanical Impedance Adjuster", Proceedings of IEEE International Conference on Robotics and Automation, 1996, vol.4, pp. 2902 – 2907.